Regular Article

LYMPHOID NEOPLASIA

Ibrutinib inhibits BCR and NF-κB signaling and reduces tumor proliferation in tissue-resident cells of patients with CLL

Sarah E. M. Herman,[1] Rashida Z. Mustafa,[1] Jennifer A. Gyamfi,[1] Stefania Pittaluga,[2] Stella Chang,[3] Betty Chang,[3] Mohammed Farooqui,[1] and Adrian Wiestner[1]

[1]Hematology Branch, National Heart, Lung and Blood Institute and [2]Laboratory of Pathology, National Cancer Institute, National Institutes of Health, Bethesda, MD; and [3]Pharmacyclics Inc., Sunnyvale, CA

Key Points

- Ibrutinib inhibits both BCR and NF-κB signaling in lymph node and bone marrow resident CLL cells.
- Rapid and sustained reduction of cellular activation and tumor proliferation was achieved in all anatomic compartments.

Chronic lymphocytic leukemia (CLL) cells depend on microenvironmental factors for proliferation and survival. In particular, tissue-resident CLL cells show prominent activation of both B-cell receptor (BCR) and NF-κB pathways. We evaluated the in vivo effects of ibrutinib, a Bruton tyrosine kinase (BTK) inhibitor on tumor cell activation and proliferation in the blood, lymph node, and bone marrow of patients with CLL. Applying validated pathway-specific gene signatures, we detected a rapid and sustained downregulation of BCR and NF-κB signaling in CLL cells from both the peripheral blood and tissue compartments during ibrutinib treatment. Ibrutinib reduced phosphorylation of PLCγ2 and ERK and decreased nuclear protein expression of NF-κB p50. Ibrutinib significantly decreased tumor proliferation and expression of surface activation markers CD69 and CD86, independent of prognostic factors such as *IGHV* mutational status, chromosome 17p deletion, or prior treatment history. Interestingly, stronger inhibition of BCR signaling in lymph node resident CLL cells after one dose of ibrutinib was associated with a higher rate of nodal response at the end of cycle 2. Together, these data validate on-target effects of BTK inhibition in the tissue compartments and demonstrate that ibrutinib effectively inhibits pathways that promote tumor cell activation and proliferation in vivo. This study is registered at www.clinicaltrials.gov as #NCT01500733. (*Blood*. 2014;123(21):3286-3295)

Introduction

Chronic lymphocytic leukemia (CLL) is characterized by the expansion of monoclonal, mature CD5^{+} B cells that proliferate in tissue compartments such as the lymph node (LN) and bone marrow (BM).[1-3] Using in vivo labeling with heavy water, the proliferation rate of CLL cells was estimated to range from 0.1% to 1% of the clone per day.[4] These differences in tumor proliferation likely account for the heterogeneous clinical course of CLL and reflect genetic differences among the malignant lymphocytes as well as the activity of external signals that drive tumor proliferation.[5]

CLL cells depend on interactions with cells and soluble factors present in the tumor microenvironment for proliferation and survival.[2,6,7] Among several pathways that may support CLL proliferation and survival in vivo, the B-cell receptor (BCR) appears to be of particular importance.[1,6,8] Antigens bound by the BCR of CLL cells include autoantigens expressed on dying cells,[9,10] as well as microbial antigens.[10-12] In vivo, the cellular response may depend on the degree to which a given BCR can interact with multiple antigens, the strength of the resulting intracellular response, and the availability of co-stimulatory signals in the tissue microenvironment. Ongoing inducible activation of BCR signaling in vivo is indicated by the finding that tissue-resident CLL cells, especially those in the LN, demonstrate more active BCR signaling than the circulating tumor cells.[1] Finally, the impressive clinical results with small molecules

that target kinases in the BCR pathway further support the importance of this pathway. In particular, inhibitors of LYN (dasatinib),[13] SYK (fostamatinib),[14] PI3Kδ (idelalisib),[15,16] and BTK (ibrutinib, CC-292)[17-20] have shown marked antitumor effects in clinical trials.

BTK, a member of the Tec family of kinases, couples BCR activation to intracellular calcium release and NF-κB signaling.[21] BTK expression is upregulated in CLL cells compared with normal B cells,[22] and its knockdown decreases the viability of primary CLL cells.[23] Furthermore, genetic ablation of BTK inhibits disease progression in mouse models of CLL, indicating its continued importance for malignant B cells.[23,24] Ibrutinib covalently binds to Cys-481 of BTK, leading to sustained inhibition of its kinase function.[25,26] Ibrutinib has been shown to be well tolerated and active across a spectrum of mature B-cell malignancies, with the highest response rates in CLL and mantle cell lymphoma.[17,27,28] In recently completed studies in CLL, the response rates with single agent were 71% in both relapsed/refractory and treatment-naïve elderly patients.[19,20]

In vitro studies demonstrated that inhibition of BTK using ibrutinib antagonizes the protective effect of stromal cells and induces a moderate degree of apoptosis.[22,29] In the Tcl1 transgenic mouse model, ibrutinib inhibited the growth of malignant (TCL1 leukemic) B cells,[29] and in a human CLL xenograft model, ibrutinib

There is an Inside *Blood* Commentary on this article in this issue.

Table 1. Patient characteristics

Patient ID	Treatment-naïve*	Rai stage	*IGHV* status†	del(17p)	CD38‡	CD49d‡	Decrease in adenopathy§
01	No	1	U	Yes	−	−	72
02	No	3	U	No	+	+	ND
03	No	4	U	Yes	+	+	71
04	No	1	M	No	−	+	51
05	No	4	U	Yes	−	+	62
06	No	4	M	No	+	+	60
07	Yes	3	U	Yes	+	−	55
08	No	4	U	No	−	+	41
09	Yes	2	U	Yes	−	−	39
10	No	4	M	Yes	+	−	43
11	Yes	1	U	Yes	−	−	60
12	No	4	U	No	+	−	64
13	No	1	U	No	+	−	89
14	No	4	U	No	+	+	53
15	No	3	U	No	+	−	76
16	Yes	4	U	Yes	−	−	74
17	No	3	U	Yes	−	+	44
18	Yes	4	M	Yes	−	−	42
19	No	4	U	Yes	+	+	49
20	Yes	4	M	No	−	−	45
21	Yes	4	M	Yes	−	+	34
22	Yes	4	M	No	+	+	49
23	No	1	M	Yes	+	−	70
–		2	M	Yes	−	−	72
25	No	4	M	No	+	+	69
26	Yes	4	U	No	−	−	58
27	Yes	2	M	No	−	+	74
28	Yes	2	M	No	−	−	45
29	No	4	U	Yes	−	+	65
30	No	4	M	Yes	−	+	51
31	Yes	1	M	Yes	−	−	53
32	No	4	M	No	+	+	42
33	No	4	U	Yes	+	+	53
34	No	3	U	No	−	+	64
35	No	4	M	Yes	−	+	56
36	No	4	U	No	+	+	45

*Among the 13 relapsed patients, the median number of prior treatments was 3 with a range of 1-7.

†Unmutated indicates <2% change in *IGHV* gene sequence compared with germline.

‡CD38 or CD49d positive (+) indicates ≥30% of CLL cells express surface antigen above isotype control.

§Decrease in lymphadenopathy was determined by the percent reduction in the sum of the product of the diameters of up to 4 lymph nodes on CT scan after 2 cycles compared with baseline. A nodal response is defined as >50% reduction. Samples that were not determined are indicated by ND.

induced apoptosis and reduced tumor proliferation and total tumor burden.[30] Correlative studies using CLL cells from the peripheral blood (PB) of patients treated with fostamatinib or ibrutinib have shown inhibition of relevant phosphoproteins and reduced expression of the proliferation marker Ki67.[31,32] However, the effects of kinase inhibitors on CLL cells residing in the tissue microenvironment, where multiple signaling pathways may be activated concurrently,[7] have not been examined. Here we analyzed the in vivo effects of ibrutinib on tumor biology in LN, BM, and circulating CLL cells from patients enrolled in a single-agent investigator-initiated study.

Methods

Patient characteristics and samples

The investigator initiated trial enrolled 2 cohorts of patients with CLL or SLL that were not well served by current standard chemoimmunotherapy: patients ≥65 years old who may experience excess toxicity and patients whose tumor cells had a deletion of the short arm of chromosome

17 (del(17p)) who have inferior responses to FCR (www.clinicaltrials.gov; NCT01500733).[33,34] Patient characteristics and nodal response at the end of cycle 2 are summarized in Table 1. Written informed consent was obtained in accordance with the Declaration of Helsinki, applicable federal regulations, and requirements of the local institutional review board. Peripheral blood samples were collected pretreatment (Pre) within 24 hours of the first dose (day 2), 2 weeks after the initiation of therapy (day 14), and at the end of cycles 1 and 2 (days 28 and 56, respectively). Lymph node core biopsies from superficial nodes deemed accessible with minimal risk were obtained both pretreatment and on day 2. When possible, single-cell suspensions were prepared and viably frozen. Bone marrow biopsy aspirates were collected both pretreatment and on day 56. Mononuclear cells were isolated by density-gradient centrifugation (Ficoll Lymphocyte Separation Media; ICN Biomedicals, Irvine, CA) and viably frozen in 90% fetal bovine serum (FBS) and 10% dimethyl sulfoxide (DMSO) (Sigma, St. Louis, MO) in liquid nitrogen.

BTK occupancy

BTK occupancy in LN core biopsies was measured using a fluorescent affinity probe (hereafter simply "probe") assay as previously described.[26] Fluorescently stained protein bands were quantified using Molecular Dynamics ImageQuant 5.2 software (GE Healthcare, Waukesha, WI). The relative

density of each band was quantified using volume integration and local average background correction as previously described.[17]

Tumor cell purification

Where indicated, purified CLL cells were used instead of mononuclear cells. Tumor cells were purified using a CD19^{+} selection with MACS Cell Separation Columns as described by the manufacturer (Miltenyi Biotec, Cambridge, MA), resulting in >96% purity (normal B cells are <1% of CD19^{+} cells).

Gene expression

Total RNA was extracted from either CD19^{+} cell pellets (PB and BM) or LN core biopsies using RNeasy kits (Qiagen, Valencia, CA), and cDNA was prepared using the High Capacity cDNA RT Kit (Applied Biosystems, Carlsbad, CA). Expression of 11 previously validated BCR and NF-κB target genes (supplemental Table 1)[1] was quantified by real-time polymerase chain reaction (RT-PCR) on TaqMan Custom Arrays (microfluidic cards) on an ABI PRISM 7900HT Sequence Detection System (Applied Biosystems). The pathway-specific signature score was determined as previously described.[1,30,32] Briefly, the difference in threshold cycle (ΔCt) for each gene of interest was calculated from the Ct of the housekeeping gene (VCP)—Ct of the gene of interest (eg, EGR1). The ΔCt for the pathway-specific genes were averaged into a signature score (5 unique genes for BCR, 5 unique genes for NF-κB, and 1 gene [CCL4] shared by both pathways).

Flow cytometry

Mononuclear cells were stained as previously described[30] with the following antibodies: anti-CD45-APC, anti-CD19-PECy5, anti-CD5-PECy7 (to identify the CLL population), and one of the following PE-conjugated antibodies: IgG1-isotype control, CD69, or CD86 (BD Biosciences, Franklin Lakes, NJ). Staining with the anti-Ki67-FITC conjugated antibody was done after surface staining. Cells were fixed with 4% paraformaldehyde (Electron Microscopy Sciences, Hatfield, PA) and permeabilized with 70% ice-cold ethyl alcohol (The Warner-Graham company, Cockeysville, MD). Analysis of phospho-protein expression was done using the BD cytofix buffer and BD phosflow perm buffer III. Cells were fixed and permeabilized according to the manufacturer's directions and stained with one of the following Alexa488-conjugated antibodies: IgG1-isotype control, anti-pPLCγ2 (Y759), or anti-pErk(T202/pY204). Cells were analyzed on a FACS Canto II flow cytometer (BD Biosciences) using FACS-DIVA 6.1.1 and FlowJo software (version 8.8.6; TreeStar, Ashland, OR).

NF-κB activity assay

NF-κB activity was measured using the TransAM NF-κB p50 transcription factor assay kit (Active Motif, Carlsbad, CA) as previously described.[35] Nuclear lysates of purified CLL cells pretreatment and on day 28 were applied to 96-well plates coated with oligonucleotides containing the NF-κB consensus sequence (5′-GGGACTTTCC-3′). Concentration of p50 was determined by comparing samples with a standard curve of purified p50 protein (Active Motif).

Immunohistochemistry

Lymph node core biopsies were fixed in 10% formalin, paraffin embedded, sectioned, and stained with hematoxylin and eosin stain (H&E) or human anti-Ki67 antibody. Images were collected using the Olympus Bx41 microscope (Center Valley, PA) at the indicated magnifications.

Statistical analysis

To compare nonrandom measurements in an individual patient either across time or compartment, a paired Student t test was used; otherwise an unpaired Student t test was used. Correlations were evaluated using the Pearson test (Prism5, GraphPad).

Results

### Ibrutinib induces rapid and sustained inhibition of BCR and NF-κB signaling in vivo

We first sought to determine the on-target effects of BTK inhibition in circulating CLL cells of patients treated with single-agent ibrutinib. BTK is essential for BCR signaling and activation of the NF-κB pathway downstream of the BCR.[21] We therefore assessed the expression of 11 genes regulated by these pathways (supplemental Table 1) by quantitative RT-PCR in purified CLL cells from the PB. As a measure of pathway activation, the mRNA levels of the respective target genes were averaged into gene signature scores. Already after one dose of ibrutinib, BCR signaling was significantly inhibited and remained suppressed throughout treatment ($P < .01$; n = 8; Figure 1A). Concurrently, ibrutinib also significantly reduced NF-κB signaling; however, the degree of NF-κB pathway inhibition increased with time on treatment through at least the first few weeks (Figure 1A). Although both BCR and NF-κB signaling were inhibited in all patients evaluated, the extent to which this occurred was highly variable (median reductions on day 28 of 81% and 74%, respectively; $P \leq .005$; n = 25; Figure 1B). This variability was not associated with any of the typical prognostic factors such as IGHV mutational status, del(17p), or previous treatment history (supplemental Figure 1). Consistent with NF-κB activation downstream of the BCR, the degree of reduction in the 2 gene signature scores was highly correlated (R = .66, $P < .001$; n = 25; Figure 1C).

Next, we assessed the phosphorylation state of proteins involved in BCR signal transduction. We first evaluated PLCγ2, a direct target of BTK. A representative histogram showing the reduction in PLCγ2 phosphorylation (pPLCγ2) on day 28 compared with pretreatment is depicted in Figure 1D. In all patients studied, circulating CLL cells showed a significant reduction in pPLCγ2 ($P < .001$; n = 30, Figure 1E). Next, we evaluated phosphorylation of ERK, an event further downstream of BCR and BTK activation, and also found a significant reduction ($P < .001$; Figure 1E). Both pPLCγ2 and pERK were reduced as early as day 2 and progressively decreased further over the first few weeks on treatment (n = 12; supplemental Figure 2). Finally, consistent with inhibition of NF-κB target gene expression, we found significantly reduced levels of NF-κB p50 in the nucleus of CLL cells on day 28 compared with pretreatment ($P = .004$; n = 10; Figure 1F). Together, these data demonstrate that ibrutinib leads to a rapid and sustained inhibition of BCR and NF-κB signaling in circulating CLL cells.

On-target effects of BTK inhibition in tissue-resident CLL cells

Both BCR and NF-κB pathways are activated in CLL cells in the tissue microenvironment.[1,6] To determine the effect of ibrutinib on tissue-resident tumor cells, we obtained matched LN core biopsies pretreatment and after one dose of ibrutinib (day 2) and BM aspirates pretreatment and after 2 cycles on drug (day 56). Using the probe assay, we detected a high degree of BTK occupancy in the LN within 24 hours, demonstrating comparable target inhibition in the tissue to what has previously been shown in peripheral blood mononuclear cells (PBMCs) (n = 6; Figure 2A).[17,19] In keeping with effective inhibition of BTK, ibrutinib significantly reduced both BCR and NF-κB target gene expression in the LN after just one dose (median reduction of respective gene signature scores by 53% and 43%, $P < .001$; n = 24; Figure 2B). Because of the rapid and substantial reduction in lymphadenopathy, a repeat LN biopsy at a later time

Figure 1. Ibrutinib induces rapid and sustained inhibition of BCR and NF-κB signaling in vivo in circulating CLL cells. (A-C) Change in BCR and NF-κB signature scores (identified in reference 1 and described in Materials and methods) in purified CLL cells on treatment. (A) Mean (± SEM) percent reduction in signature scores (n = 8 patients, in whom all time points were available). Comparisons by paired Student t test: *P < .05, **P < .01, and ***P < .001. (B) Percent reduction on day 28 compared with pretreatment. Each dot represents a different patient (n = 25). The line represents the median. (C) Correlation of reduction in BCR and NF-κB signature scores. Each dot represents one patient. R and P values of Pearson correlation are displayed (n = 25). (D-E) PBMCs were fixed, permeabilized, and stained with the indicated antibody. Results shown are for the CLL population (CD5$^+$/CD19$^+$). (D) A representative histogram of pPLCγ2 staining. Isotype control is represented by the gray shaded area, the dashed line represents pretreatment, and the solid black line day 28. (E) The mean (± SEM) percent of pPLCγ2 and pERK expressing CLL cells pretreatment (Pre) and on day 28 of ibrutinib treatment is shown (n = 30). (F) Quantification of nuclear p50 was done on nuclear lysates from CLL cells pretreatment (Pre) and on day 28 of ibrutinib treatment (n = 10).
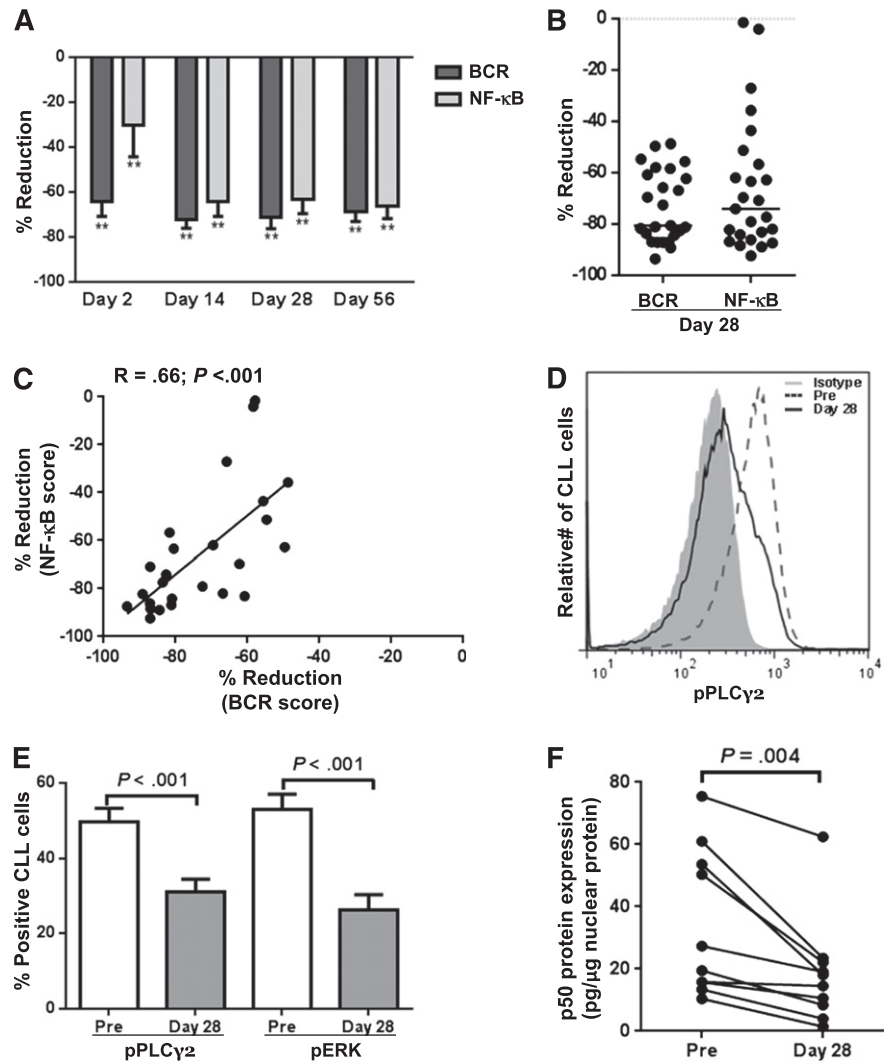
point was not practical. We therefore analyzed purified CLL cells obtained from BM aspirates on day 56 and again found sustained inhibition of both BCR and NF-κB signaling (median reduction in the respective scores 73% and 68%, P < .05; n = 8; Figure 2C). Although every patient evaluated demonstrated a reduction in the tissue compartment of both gene signature scores, there was substantial interpatient variability. As was already shown for circulating CLL cells, this variability was not correlated with *IGHV* mutational status, presence of del(17p), or previous treatment history (supplemental Figures 3 and 4) but the reductions in BCR and NF-κB scores were also strongly correlated in both LN (R=.77, P < .001; n = 24, Figure 2D) and BM resident CLL cells (data not shown).

Tissue-resident CLL cells also showed a significant reduction in pPLCγ2 (P = .02; n = 8, and P = .005; n = 10, for LN and BM, respectively; Figure 2E) and pERK (P = .05, LN and P = .004, BM; Figure 2F). Pretreatment, the proportion of CLL cells having detectable levels of the activated signaling molecules was higher in the LN than in the BM and the reduction on treatment, although significant in both tissues, appeared to be more pronounced in the BM samples. However, this is likely because of the difference in time points analyzed because the repeat measurement in the LN was taken after just one dose of drug (day 2), whereas the BM cells were reanalyzed after 2 complete cycles of therapy. Interestingly, both pPLCγ2 and pERK were substantially reduced in CLL cells aspirated

from the BM at 2 months (P ≤ .005). Thus, ibrutinib effectively inhibits BCR and NF-κB signaling not only in circulating cells but also in tumor cells within the tissue microenvironment.

Ibrutinib inhibits activation and proliferation of CLL cells in vivo

We next assessed the effect of ibrutinib on cellular activation as reflected in the expression of cell surface markers on circulating CLL cells. After just one dose, there was a modest but significant reduction in CD69, a classic lymphocyte activation marker (P < .05; n = 20; Figure 3A), paralleled by a more pronounced downregulation of CD86, an activation marker regulated by NF-κB (P < .001; n = 20; Figure 3B). Expression of both markers decreased further over the subsequent weeks, and a reduction in cellular activation was seen in all but one evaluated patient at the end of cycle 1, albeit with considerable interpatient variability (P < .001; n = 30; Figure 3C-D).

Similarly, both CD69 and CD86 expression was also significantly reduced in tissue-resident CLL cells (P ≤ .02; n = 8 for LN and n = 10 for BM; Figure 3E-F). Consistent with our gene expression data, baseline expression of both activation markers was stronger in CLL cells isolated from the LN than from the BM. Consistent with what we observed in the PB, we again see that both markers were rapidly and sustainably downregulated by ibrutinib in
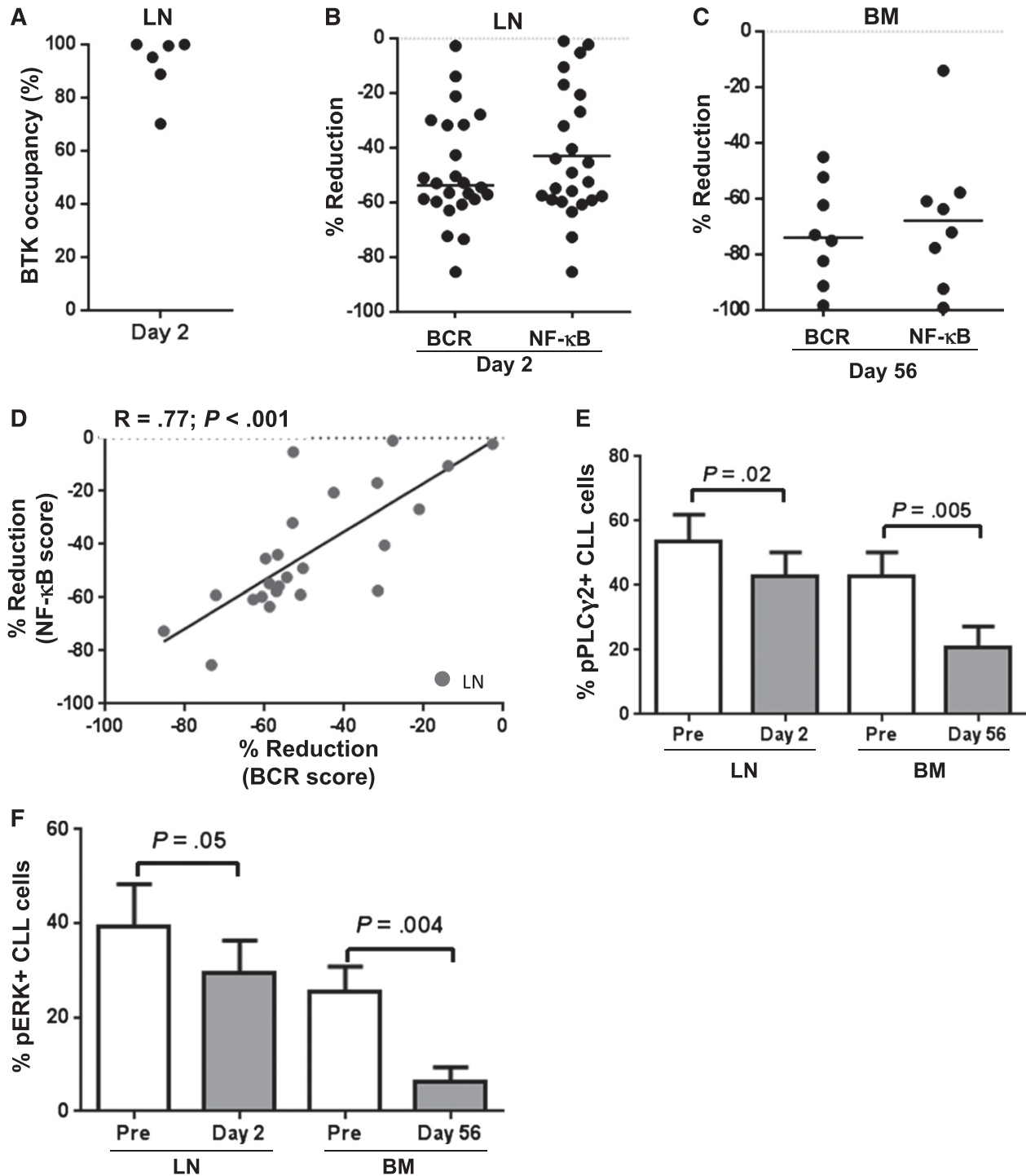
Figure 2. Ibrutinib has a strong on-target effect in tissue-resident CLL cells. (A) BTK occupancy in lymph node (LN) biopsies on day 2 compared with pretreatment as determined by probe assay. Each dot represents a different patient (n = 6). (B-C) Percent reduction in BCR and NF-κB signature scores in either (B) LN biopsies (n = 24) or (C) CLL cells purified from bone marrow (BM) aspirates (n = 8). The line represents the median. (D) Correlation of reduction in BCR and NF-κB signature scores in LN biopsies (n = 24). (E-F) Mononuclear cells from LN biopsies (n = 8) or BM aspirates (n = 10) were fixed, permeabilized, and stained with the indicated antibody. Results shown are for the CLL population (CD5$^+$/CD19$^+$). The mean (± SEM) percent of (E) pPLCγ2 and (F) pERK expressing CLL cells pretreatment (Pre) and on ibrutinib is shown.

the tissue compartment, as seen on day 2 in the LN and after 2 cycles in the BM. Together these data show inhibition of tumor cell activation in a time-dependent manner that appears to affect the tumor cells in all tissues analyzed.

Consistent with our prior study, the average rate of Ki67$^+$ CLL cells pretreatment was higher in the LN (18%) than in the BM (9%) and PB (3%).[1] Figure 4A shows a representative histogram

demonstrating the reduction in Ki67 staining on ibrutinib. Ki67 staining in CLL cells in the LN was already significantly reduced within 24 hours of the first dose (n = 8, $P = .02$), and was almost completely lost in the BM at the end of the second cycle ($P = .003$; n = 10; Figure 4B). Histologic sections of LN on day 2 compared with pretreatment were consistent with a moderate reduction in Ki67$^+$ cells at this early time point (Figure 4C). Ki67$^+$ cells in circulation,

Figure 3. Ibrutinib inhibits cellular activation. (A-B) The percentage of CLL cells expressing the cell surface marker (A) CD69 and (B) CD86 on CLL cells from peripheral blood (PB, n = 20) was compared between pretreatment (Pre) and various treatment time points. Comparisons by paired Student t test: *P < .05, **P < .01, and ***P < .001. (C-D) The percentage of CLL cells expressing the cell surface marker (C) CD69 and (D) CD86 on CLL cells from PB (n = 30) was compared between pretreatment (Pre) and day 28. Comparisons are by paired Student t test. (E-F) Mononuclear cells from lymph node biopsies (LN, n = 8) or bone marrow (BM) aspirates (n = 10) were stained with the indicated antibody. Results shown are for the CLL population (CD5$^+$/CD19$^+$). The mean (± SEM) percent of (E) CD69 and (F) CD86 expressing CLL cells pretreatment (Pre) and on ibrutinib is shown. Comparisons are by paired Student t test.
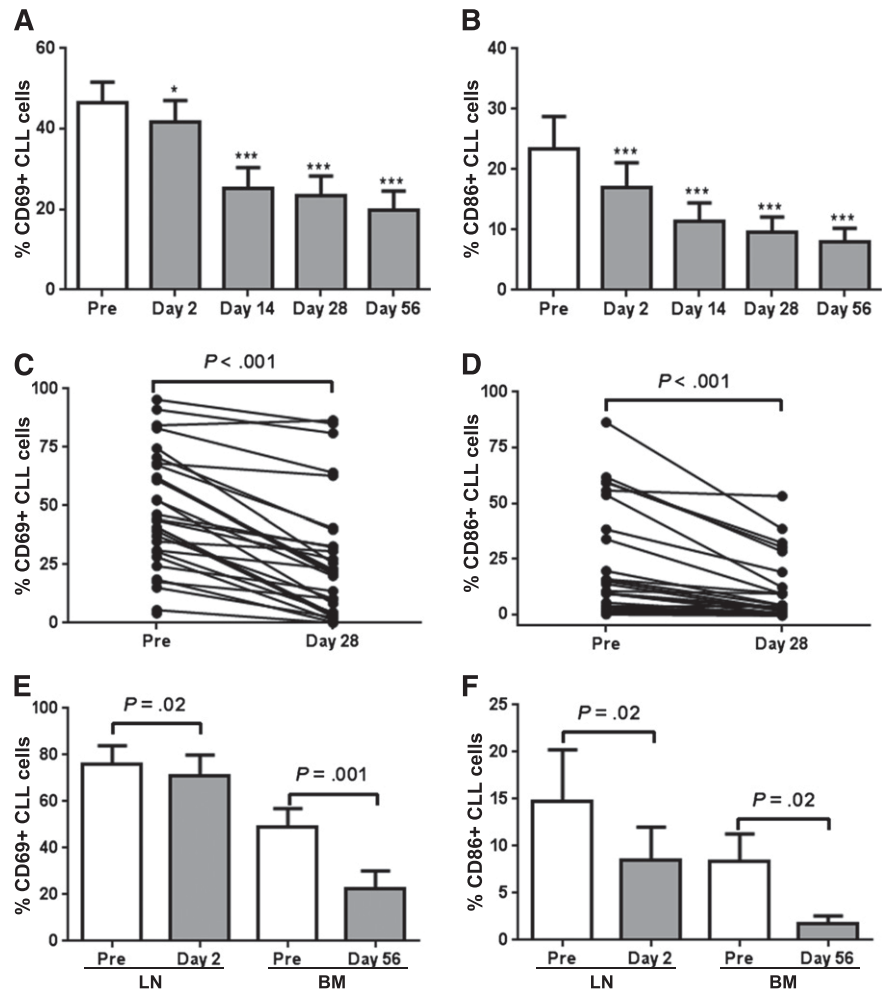
although already infrequent at baseline (<2.5% median expression), approached undetectable levels (<0.5% median expression) on treatment (n = 20; Figure 4D). Thus, ibrutinib greatly inhibits tumor proliferation in both the LN and BM tissue microenvironment in vivo.

Nodal response, clinical characteristics, and inhibition of BCR signaling

Except for one, all patients had a response assessment by computed tomography scan at 2 months on therapy. The nodal response was calculated as the percent reduction in the sum of the product of the diameters of up to 4 LNs (Table 1). The median reduction at 2 months was 55% (range 34%-76%), and 66% of patients achieved a >50% reduction in lymphadenopathy. The degree of nodal response was not correlated to any of the clinical or prognostic markers assessed; in particular there was no difference by del(17p) or *IGHV* gene mutation status (Table 1).

Next we tested whether the degree of inhibition of BCR signaling correlated with nodal response. In 23 patients, paired LN biopsies pretreatment and on day 2 after one dose of ibrutinib were available. Reflecting activation of BCR signaling in CLL cells in the LN, the BCR signature score was higher in LN biopsies than in circulating CLL cells for patients with both mutated and unmutated *IGHV* (P = .003 and P = .001, respectively; Figure 5A). The baseline BCR score in the LN was not statistically different between *IGHV*-mutated and unmutated tumor cells. This appears to be caused by considerable

variability in the *IGHV* mutated group. Notwithstanding the pretreatment difference, the degree of reduction in the BCR score on ibrutinib was equal for both subtypes (Figure 5B). The BCR gene signature score on treatment was reduced by >50% from baseline in 14 patients and all but one of these patients (93%) had a nodal response (ie, >50% reduction in adenopathy) at 2 months (Figure 5C). In contrast, the nodal response rate in patients with ≤50% reduction in the BCR score was 44% (P = .01). The degree of reduction in lymphadenopathy was also significantly different between the 2 groups (P = .01; Figure 5C-D). In circulating cells, the BCR signature score on day 2 was already reduced >50% in all but one patient, and there was no correlation with nodal response.

Discussion

The BTK inhibitor ibrutinib has recently been shown to have robust clinical activity in CLL.[20,36] In vitro, ibrutinib disrupts pathways involved in tumor-microenvironment interactions but induces only a moderate degree of apoptosis.[22,29,31] Here, we characterized the treatment-induced effects on CLL cells in the tissue microenvironment of patients treated with single-agent ibrutinib. Ibrutinib effectively inhibited BCR and NF-κB signaling in CLL cells in LN, BM, and PB. Activity of the signaling pathways was estimated from the expression of representative target genes as done in previous studies[1,32,37-40] and
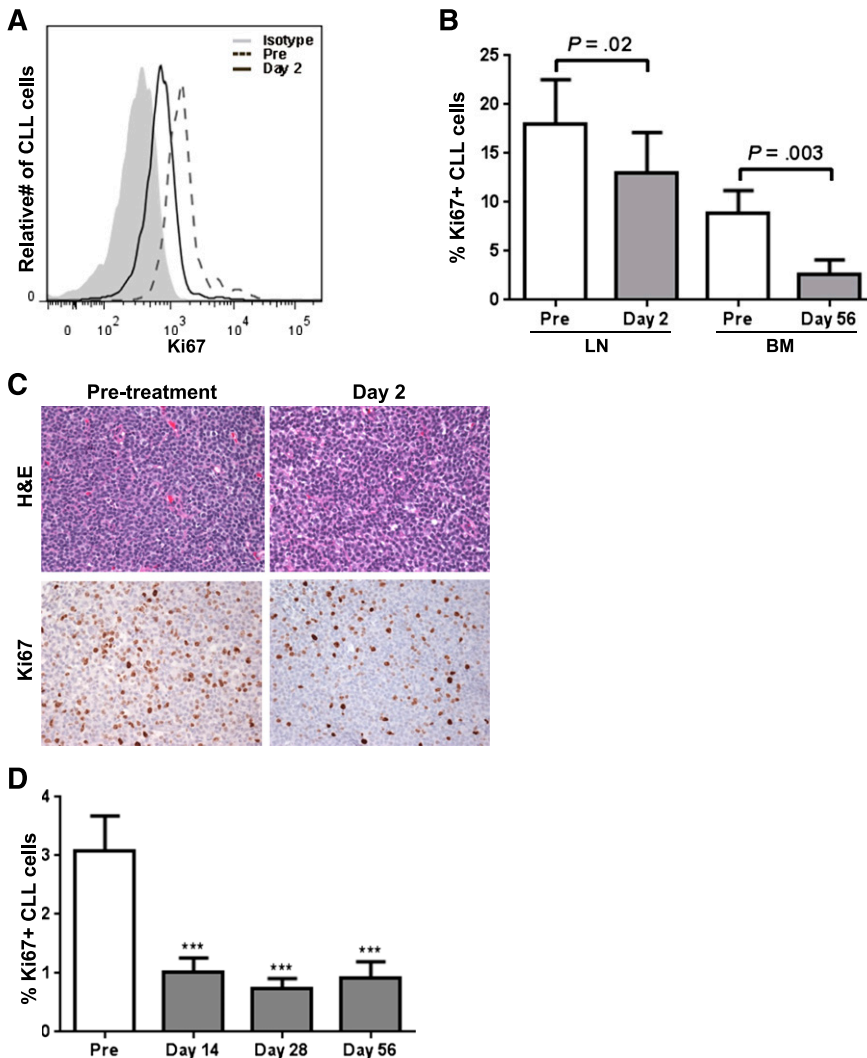
Figure 4. Ibrutinib inhibits tumor proliferation in lymph node and bone marrow. (A) A representative histogram of Ki67 staining on CLL cells in the lymph node (LN). Isotype control is represented by the gray shaded area, the dashed line represents pretreatment, and the solid black line day 2. (B) Mononuclear cells from LN (n = 8) or bone marrow (BM) aspirates (n = 10) were fixed, permeabilized, and stained with the indicated antibody. Results shown are for the CLL population (CD5$^+$/CD19$^+$). The mean (± SEM) percent of Ki67 expressing CLL cells pretreatment and on ibrutinib is shown. Comparisons are by paired Student t test. (C) Images of LN tissue obtained pretreatment and on day 2 of ibrutinib stained with hematoxylin and eosin (H&E) and anti Ki67 were captured at ×40 magnification on an Olympus Bx41 microscope. (D) The percent of CLL cells expressing Ki67 at various clinical time points in the PB is shown (n = 20). Significance compared with pretreatment was determined by a paired Student t test and is indicated by asterisks: ***$P <$ .001.

corroborated with flow cytometry for activated signaling molecules and quantification of nuclear NF-κB p50. The onset of these on-target effects was rapid as demonstrated in the LN and sustained as shown in the BM and PB. Although BTK and its direct target PLCγ2 are essential for BCR-dependent NF-κB activation, additional pathways may cooperate with the BCR to activate NF-κB, including toll-like receptors, CD40 ligation, and B-cell activating factor (BAFF).[41-44] To variable degrees, these pathways can also be inhibited by ibrutinib.[22,45,46] Interestingly, maximum inhibition of BCR signaling was already achieved with only one dose of drug, whereas maximum inhibition of NF-κB required repeat dosing. Similarly, after the first dose of ibrutinib pPLCγ2 (a direct target of BTK) and pERK (a protein downstream of multiple signaling pathways) were decreased to a comparable degree, whereas the reduction in phosphorylation after repeat dosing was more pronounced for ERK than for PLCγ2. Together, this may indicate that not all effects of ibrutinib are direct and that continued treatment may lead to changes in the microenvironment that could have secondary effects on the tumor cells. Given the recently appreciated effect of ibrutinib on T cells through inhibition of ITK and a possible effect on monocytes/macrophages through inhibition of TEC kinase,[47,48] this hypothesis deserves further study. However, it is notable that the first recognized mechanism of resistance to ibrutinib are mutations in BTK that lead to loss of Cysteine 481 (C481S), the amino acid necessary for covalent binding of ibrutinib.[49] These data

together with the on-target effects shown here suggest that BTK is indeed a central signaling node mediating the nourishing and protective effects of the tumor microenvironment.

It is well appreciated that ibrutinib leads to a transient increase in circulating CLL cells concurrent with the reduction in lymphadenopathy.[17,20,36] In accordance with this, we observed a rise in absolute lymphocyte count and a reduction in lymphadenopathy on treatment in all patients. Thus, shifts in disease distribution may contribute to changing characteristics of tumor cells. We recently reported that the onset of treatment-induced lymphocytosis is within hours of starting ibrutinib and that, consistent with the efflux of activated cells from the tissue compartments, there is an increase in Ki67 expressing CLL cells in circulation.[50] On continued treatment, we and others show that the frequency of Ki67-expressing cells in circulation is greatly reduced.[23,31] Whether this reflects inhibition of tumor proliferation in tissue sites or an inability of the circulating cells to home into the LNs and BM has not been addressed in patient samples. Here we show direct evidence for consistent and sustained inhibition of tumor proliferation in the tissue microenvironment. A reduction in tumor proliferation was apparent after just one dose of drug in the LN. Repeat sampling of LNs at later time points was not feasible, in large part because of the rapid reduction in lymphadenopathy. However, we observed sustained inhibition of proliferation in CLL cells obtained from the BM at the end of cycle 2. In BM

Figure 5. Inhibition of BCR signaling in the LN correlates with nodal response. (A-B) BCR gene signature scores are shown for patients with mutated (n = 9) and unmutated *IGHV* (n = 14). Comparisons within patients are by paired Student *t* test, whereas comparisons between mutational subgroups are by an unpaired Student *t* test. (A) Comparison of baseline BCR scores in CLL cells sampled from the peripheral blood (PB) and the matching lymph node (LN). (B) Comparison of pretreatment and day 2 BCR scores in LN core biopsies. (C) Correlation between percent reduction in lymphadenopathy and percent reduction in BCR signaling on day 2 in the lymph node. Gray squares represent patients who did not achieve a 50% reduction in lymphadenopathy after 2 months on treatment. Dashed lines represent the 50th percentile. (D) Percent reduction in lymphadenopathy in patients divided by the degree of reduction in the BCR signature score. Comparison is by Student *t* test.
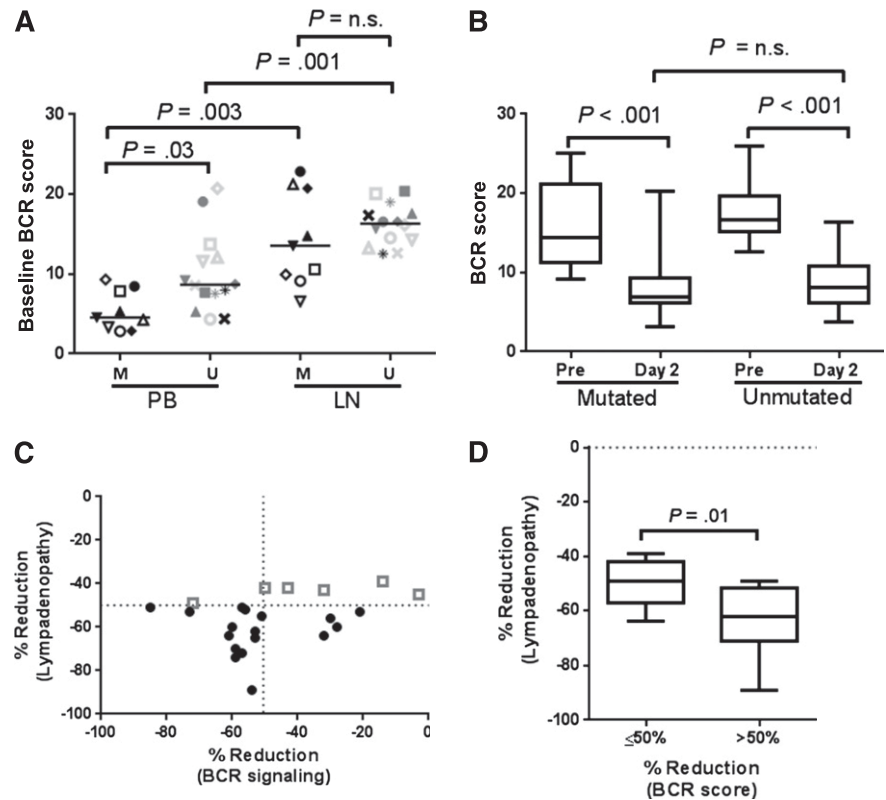
aspirates, we found a decrease of >70% in the frequency of Ki67$^+$ cells at 2 months compared with baseline. Consistently, we noted that proliferation centers often present in pretreatment biopsies were consistently absent from on-treatment biopsies (data not shown).

Ibrutinib has been reported to induce dose-dependent apoptosis in vitro.[22,29] However, even in vitro, the degree of apoptosis at drug concentrations achieved in vivo is modest.[22,31] Similarly, Cheng et al found no consistent increase in the rate of apoptosis of circulating CLL cells in their patients.[31] The absence of overt cytotoxic effects, although consistent with the absence of clinical reports on tumor lysis syndrome, contrasts with the potent inhibition of survival pathways and the substantial reduction of cellular proliferation. The often rapid and substantial reductions in tumor burden appear difficult to explain merely by reduced proliferation, and inhibition of survival mechanisms downstream of NF-κB likely results in some increased attrition of cells. Consistent with this notion, we previously reported a slight increase in the number of dead or dying cells in fresh whole blood samples of patients on ibrutinib, as well as a reduced viability of xenografted human CLL cells in the spleens of NSG mice treated with ibrutinib.[30]

Finally, we tested whether effective inhibition of signaling pathways correlated with antitumor response. Interestingly, nodal responses at 2 months were superior in patients who achieved a >50% reduction in the BCR score after the first dose of drug. In this analysis, we included all 23 patients who provided matched LN biopsies pretreatment and on day 2. In contrast, reduction in the BCR score in circulating cells was not correlated to nodal response. In addition, there was no correlation between nodal response and clinical characteristics, such as *IGHV* mutation status, or del(17p). Although a slower resolution of treatment-induced lymphocytosis in patients with *IGHV* mutated compared with unmutated CLL has been described,[19,46] we found no significant difference between the *IGHV*

subgroups in regards to on-target effects of ibrutinib. Thus, the basis for the observed variability in the inhibition of BCR signaling in the LN remains to be defined. Next we divided the patients into two groups based on whether the BCR signature score was reduced >50% or not. The nodal response rate at 6 months was 94% in patients with >50% reduction in the BCR score, and 44% in the remaining patients (*P* = .01). It is notable that all patients in this study had a reduction in lymphadenopathy; thus future correlation to progression-free survival will be important. Nonwithstanding, these data provide a first indication of a link between the strength of on-target effects and tumor response. Future studies are needed to validate these observations, investigate whether surrogate markers of pathway inhibition can serve as predictors of response, and investigate the molecular basis for differential responses to ibrutinib.

In summary, on-target effects of ibrutinib in vivo include inhibition of critical signaling pathways in particular BCR and NF-κB, and decreased CLL cell activation, proliferation, and likely survival in blood, BM, and LN. Extending these analyses to patients progressing on treatment will be important to unveil mechanisms of resistance and possible limitations of single-agent therapy.

Acknowledgments

Authorship

Contribution: S.E.M.H. planned the research, performed experiments, and analyzed data; R.Z.M., S.B., and B.C. were involved in planning components of the research and supported experiments; J.A.G. determined IGHV mutational status of all patients; S.P. analyzed histologic samples; A.W. planned and supervised the research; M.F. and A.W. implemented the clinical trial; S.E.M.H. and A.W. wrote the paper; and all authors approved the final version of the manuscript.

Conflict-of-interest disclosure: S.C. and B.C. are employees of Pharmacyclics Inc. and have financial interest in the development of ibrutinib. The remaining authors declare no competing financial interests.

Correspondence: Adrian Wiestner, Hematology Branch, NHLBI, NIH, Bldg 10, CRC 3-5140, 10 Center Dr, Bethesda, MD 20892-1202; e-mail: adrian.wiestner@nih.gov.

References

1. Herishanu Y, Pérez-Galán P, Liu D, et al. The lymph node microenvironment promotes B-cell receptor signaling, NF-kappaB activation, and tumor proliferation in chronic lymphocytic leukemia. *Blood*. 2011;117(2):563-574.

2. Burger JA. Nurture versus nature: the microenvironment in chronic lymphocytic leukemia. *Hematol Am Soc Hematol Educ Program*. 2011;2011:96-103.

3. Chiorazzi N, Rai KR, Ferrarini M. Chronic lymphocytic leukemia. *N Engl J Med*. 2005;352(8):804-815.

4. Messmer BT, Messmer D, Allen SL, et al. In vivo measurements document the dynamic cellular kinetics of chronic lymphocytic leukemia B cells. *J Clin Invest*. 2005;115(3):755-764.

5. Rossi D, Spina V, Bomben R, et al. Association between molecular lesions and specific B-cell receptor subsets in chronic lymphocytic leukemia. *Blood*. 2013;121(24):4902-4905.

6. Ghia P, Chiorazzi N, Stamatopoulos K. Microenvironmental influences in chronic lymphocytic leukaemia: the role of antigen stimulation. *J Intern Med*. 2008;264(6):549-562.

7. Herishanu Y, Katz BZ, Lipsky A, Wiestner A. Biology of chronic lymphocytic leukemia in different microenvironments: clinical and therapeutic implications. *Hematol Oncol Clin North Am*. 2013;27(2):173-206.

8. Stevenson FK, Krysov S, Davies AJ, Steele AJ, Packham G. B-cell receptor signaling in chronic lymphocytic leukemia. *Blood*. 2011;118(16):4313-4320.

9. Chu CC, Catera R, Hatzi K, et al. Chronic lymphocytic leukemia antibodies with a common stereotypic rearrangement recognize nonmuscle myosin heavy chain IIA. *Blood*. 2008;112(13):5122-5129.

10. Lanemo Myhrinder A, Hellqvist E, Sidorova E, et al. A new perspective: molecular motifs on oxidized LDL, apoptotic cells, and bacteria are targets for chronic lymphocytic leukemia antibodies. *Blood*. 2008;111(7):3838-3848.

11. Steininger C, Widhopf GF II, Ghia EM, et al. Recombinant antibodies encoded by IGHV1-69 react with pUL32, a phosphoprotein of cytomegalovirus and B-cell superantigen. *Blood*. 2012;119(10):2293-2301.

12. Hoogeboom R, van Kessel KP, Hochstenbach F, et al. A mutated B cell chronic lymphocytic leukemia subset that recognizes and responds to fungi. *J Exp Med*. 2013;210(1):59-70.

13. Amrein PC, Attar EC, Takvorian T, et al. Phase II study of dasatinib in relapsed or refractory chronic lymphocytic leukemia. *Clin Cancer Res*. 2011; 17(9):2977-2986.

14. Friedberg JW, Sharman J, Sweetenham J, et al. Inhibition of Syk with fostamatinib disodium has significant clinical activity in non-Hodgkin lymphoma and chronic lymphocytic leukemia. *Blood*. 2010;115(13):2578-2585.

15. Coutre SE, Byrd JC, Furman RR, et al. Phase I study of CAL-101, an isoform-selective inhibitor of phosphatidylinositol 3-kinase P110d, in patients with previously treated chronic lymphocytic leukemia. *J Clin Oncol*. 2011;29(suppl): abstr 6631.

16. Furman RR, Sharman JP, Coutre SE, et al. Idelalisib and rituximab in relapsed chronic lymphocytic leukemia. *N Engl J Med*. 2014; 370(11):997-1007.

17. Advani RH, Buggy JJ, Sharman JP, et al. Bruton tyrosine kinase inhibitor ibrutinib (PCI-32765) has significant activity in patients with relapsed/refractory B-cell malignancies. *J Clin Oncol*. 2013; 31(1):88-94.

18. Brown JR, Harb W, Sharman J, et al. Phase 1 study of single agent CC-292, a highly selective Bruton's tyrosine kinase (BTK) inhibitor, in relapsed/refractory chronic lymphocytic leukemia (CLL) and B-cell non-Hodgkin lymphoma (B-NHL). *Haematologica*. 2013;98(s1):S520.

19. Byrd JC, Furman RR, Coutre SE, et al. Targeting BTK with ibrutinib in relapsed chronic lymphocytic leukemia. *N Engl J Med*. 2013;369(1):32-42.

20. O'Brien S, Furman RR, Coutre SE, et al. Ibrutinib as initial therapy for elderly patients with chronic lymphocytic leukaemia or small lymphocytic lymphoma: an open-label, multicentre, phase 1b/2 trial. *Lancet Oncol*. 2014;15(1):48-58.

21. Buggy JJ, Elias L. Bruton tyrosine kinase (BTK) and its role in B-cell malignancy. *Int Rev Immunol*. 2012;31(2):119-132.

22. Herman SE, Gordon AL, Hertlein E, et al. Bruton tyrosine kinase represents a promising therapeutic target for treatment of chronic lymphocytic leukemia and is effectively targeted by PCI-32765. *Blood*. 2011;117(23):6287-6296.

23. Woyach JA, Bojnik E, Ruppert AS, et al. Bruton's tyrosine kinase (BTK) function is important to the development and expansion of chronic lymphocytic leukemia (CLL). *Blood*. 2014; 123(8):1207-1213.

24. Kil LP, de Bruijn MJ, van Hulst JA, Langerak AW, Yuvaraj S, Hendriks RW. Bruton's tyrosine kinase mediated signaling enhances leukemogenesis in a mouse model for chronic lymphocytic leukemia. *Am J Blood Res*. 2013;3(1):71-83.

25. Pan Z, Scheerens H, Li SJ, et al. Discovery of selective irreversible inhibitors for Bruton's tyrosine kinase. *ChemMedChem*. 2007;2(1):58-61.

26. Honigberg LA, Smith AM, Sirisawad M, et al. The Bruton tyrosine kinase inhibitor PCI-32765 blocks B-cell activation and is efficacious in models of autoimmune disease and B-cell malignancy. *Proc Natl Acad Sci USA*. 2010;107(29):13075-13080.

27. Wang ML, Rule S, Martin P, et al. Targeting BTK with ibrutinib in relapsed or refractory mantle-cell lymphoma. *N Engl J Med*. 2013; 369(6):507-516.

28. Wiestner A. Targeting B-Cell receptor signaling for anticancer therapy: the Bruton's tyrosine kinase inhibitor ibrutinib induces impressive responses in B-cell malignancies. *J Clin Oncol*. 2013;31(1):128-130.

29. Ponader S, Chen SS, Buggy JJ, et al. The Bruton tyrosine kinase inhibitor PCI-32765 thwarts chronic lymphocytic leukemia cell survival and tissue homing in vitro and in vivo. *Blood*. 2012; 119(5):1182-1189.

30. Herman SE, Sun X, McAuley EM, et al. Modeling tumor-host interactions of chronic lymphocytic leukemia in xenografted mice to study tumor biology and evaluate targeted therapy. *Leukemia*. 2013;27(12):2311-2321.

31. Cheng S, Ma J, Guo A, et al. BTK inhibition targets in vivo CLL proliferation through its effects on B-cell receptor signaling activity. *Leukemia*. 2014;28(3):649-657.

32. Herman SE, Barr PM, McAuley EM, Liu D, Wiestner A, Friedberg JW. Fostamatinib inhibits B-cell receptor signaling, cellular activation and tumor proliferation in patients with relapsed and refractory chronic lymphocytic leukemia. *Leukemia*. 2013;27(8):1769-1773.

33. Farooqui M, Aue G, Valdez J, et al. Single Agent Ibrutinib (PCI-32765) Achieves Equally Good and Durable Responses In Chronic Lymphocytic Leukemia (CLL) Patients With and Without Deletion 17p. *Blood*. 2013; 122(21):673.

34. Hallek M, Fischer K, Fingerle-Rowson G, et al; International Group of Investigators; German Chronic Lymphocytic Leukaemia Study Group. Addition of rituximab to fludarabine and cyclophosphamide in patients with chronic lymphocytic leukaemia: a randomised, open-label, phase 3 trial. *Lancet*. 2010;376(9747):1164-1174.

35. Dühren-von Minden M, Übelhart R, Schneider D, et al. Chronic lymphocytic leukaemia is driven by antigen-independent cell-autonomous signalling. *Nature*. 2012;489(7415):309-312.

36. Byrd JC, O'Brien S, James DF. Ibrutinib in relapsed chronic lymphocytic leukemia. *N Engl J Med*. 2013;369(13):1278-1279.

37. Pérez-Galán P, Mora-Jensen H, Weniger MA, et al. Bortezomib resistance in mantle cell lymphoma is associated with plasmacytic differentiation. *Blood*. 2011;117(2):542-552.

38. Weniger MA, Rizzatti EG, Pérez-Galán P, et al. Treatment-induced oxidative stress and cellular antioxidant capacity determine response to bortezomib in mantle cell lymphoma. *Clin Cancer Res*. 2011;17(15):5101-5112.

39. Davis RE, Ngo VN, Lenz G, et al. Chronic active B-cell-receptor signalling in diffuse large B-cell lymphoma. *Nature*. 2010;463(7277):88-92.

40. Lam LT, Davis RE, Pierce J, et al. Small molecule inhibitors of IkappaB kinase are selectively toxic

for subgroups of diffuse large B-cell lymphoma defined by gene expression profiling. *Clin Cancer Res.* 2005;11(1):28-40.

41. Endo T, Nishio M, Enzler T, et al. BAFF and APRIL support chronic lymphocytic leukemia B-cell survival through activation of the canonical NF-kappaB pathway. *Blood.* 2007;109(2): 703-710.

42. Muzio M, Bertilaccio MT, Simonetti G, Frenquelli M, Caligaris-Cappio F. The role of toll-like receptors in chronic B-cell malignancies. *Leuk Lymphoma.* 2009;50(10):1573-1580.

43. Ying H, Li Z, Yang L, Zhang J. Syk mediates BCR- and CD40-signaling integration during B cell activation. *Immunobiology.* 2011;216(5):566-570.

44. Cancro MP. Signalling crosstalk in B cells: managing worth and need. *Nat Rev Immunol.* 2009;9(9):657-661.

45. Wiestner A. Emerging role of kinase-targeted strategies in chronic lymphocytic leukemia. *Blood.* 2012;120(24):4684-4691.

46. Woyach JA, Smucker K, Smith LL, et al. Prolonged lymphocytosis during ibrutinib therapy is associated with distinct molecular characteristics and does not indicate a suboptimal response to therapy. *Blood.* 2014;123(12): 1810-1817.

47. Dubovsky JA, Beckwith KA, Natarajan G, et al. Ibrutinib is an irreversible molecular inhibitor of ITK driving a Th1-selective pressure in

T lymphocytes. *Blood.* 2013;122(15): 2539-2549.

48. Koprulu AD, Ellmeier W. The role of Tec family kinases in mononuclear phagocytes. *Crit Rev Immunol.* 2009;29(4):317-333.

49. Chang BY, Furman RR, Zapatka M, et al. Use of tumor genomic profiling to reveal mechanisms of resistance to the BTK inhibitor ibrutinib in chronic lymphocytic leukemia (CLL). *J Clin Oncol.* 2013; 31(suppl 1):7014.

50. Herman SEM, Carsten NU, Farooqui M, et al. Ibrutinib-induced lymphocytosis in patients with chronic lymphocytic leukemia: correlative analyses from a phase II study [published online ahead of print April 4, 2014]. *Leukemia.* doi: 10.1038/leu.2014.122.